

Universal shape characteristics for the mesoscopic star-shaped polymer *via* dissipative particle dynamics simulations

O. Kalyuzhnyi^{1,4}, J.M. Ilnytskyi^{1,4}, Yu.Holovatch^{1,4}

C. von Ferber^{2,3,4}

¹Institute for Condensed Matter Physics, National Academy of Sciences of Ukraine, UA-79011 Lviv, Ukraine

²Applied Mathematics Research Centre, Coventry University, Coventry, CV1 5FB, United Kingdom

³Heinrich-Heine Universität Düsseldorf, D-40225 Düsseldorf, Germany

⁴L⁴ Collaboration & Doctoral College for the Statistical Physics of Complex Systems, Leipzig-Lorraine-Lviv-Coventry, D-04009 Leipzig, Germany

Abstract. In this paper we study the shape characteristics of star-like polymers in various solvent quality using a mesoscopic level of modeling. The dissipative particle dynamics simulations are performed for the homogeneous and four different heterogeneous star polymers with the same molecular weight. We analyse the gyration radius and asphericity at the bad, good and θ -solvent regimes. Detailed explanation based on interplay between enthalpic and entropic contributions to the free energy and analyses on of the asphericity of individual branches are provided to explain the increase of the asphericity in θ -solvent regime.

PACS numbers: 61.25Hq, 61.20.Ja, 89.75.Da

Keywords: star-like polymer, θ -solvent, dissipative particle dynamics

Submitted to: *J. Phys.: Condens. Matter*

1. Introduction

Star polymers represent the simplest case of branched polymers, consisting of f linear chains connected to the central core. The central core can be an atom, or a molecule or even a macromolecule. The first synthesis of star polymers was made by Shaefgen and Flory [1] in 1948. More than ten years later Morton *et al.* [2] have synthesized the 3- and 4-branch polystyrene stars. Since then the methods of synthesis have been drastically improved. Currently, there are several general methods to synthesis star polymers: using multifunctional linking agents or multifunctional initiators and via difunctional monomers [3, 4]. There are several important polymerization techniques, i.e. cationic, anionic, controlled radical, ring opening, group transfer, step-growth polycondensation and their combinations (see Ref. [5] and references therein). Substantial interest in theoretical and experimental studies of star polymers arises due to their important applications. by their practical applications importance. Star polymers may have a properties much different from those of the linear chain polymers. They have more compact size and, therefore, higher segment density compared to their linear counterparts with the same molecular weight. This feature affects substantially the properties of the star polymer containing systems [3, 4]. Their bulk viscosity in concentrated as well as in dilute solution, can be lower than for a linear polymers of similar molecular weight. Besides that star polymers can self-assemble in more types of microstructures, which can be promoted in solutions due to the presence of the functional groups in their branches, or by using a selective solvent in the case of star-block or miktoarm star copolymers, leading to the formation of micellar structures [6].

In terms of molecular topology, star polymers represent an intermediate system between linear chain polymers and colloidal particles such as polystyrene and silica spheres. This feature has been discussed in a number of papers, in which the structure [7–10] and dynamics [11–19] of the star polymers have been studied. The properties of the stars with a small number of branches are similar to those of the linear chain polymers. In particular, their average configuration is characterized by a large asphericity [20, 21]. The star structures with larger number of the branches have much lower asphericity and in the limit of large f they can be seen as rigid spherical particles [22]. Star polymers have substantially higher shear stability [23] and they are widely used as viscosity index modifier in the multigrade lubricating oils [24, 25]. They are also used for manufacturing the thermoplastic elastomers, which at room temperature have the properties similar to those of cross-linked elastomers (such as vulcanized rubber). However, with the temperature increase, they became soft and can flow, which is a very useful property for their processing [26]. In addition, thermoplastic elastomers, in contrast to rubber, can be reused. For producing thermoplastic elastomers the mixture of linear and miktoarm star triblock copolymers is often used [26]. Star polymer systems are used in coating materials, as binders for toners for copying machines [8], resins for electrophotographic photoreceptors [27] and in a number of pharmaceutical and medical applications [8, 28]. Star polymers and starburst dendrimers also have

important applications in semiconductor devices [29], in biofunctionalized patterning of the surfaces [30], and in controlled release drug delivery [31]. Reviews of the synthesis, properties and applications of star polymers are given in Ref. [5].

Due to the substantial advances in the synthesis of star polymers, as well as their numerous applications, they have attracted considerable interest both theoretical and experimental methods [3–6,8]. Theoretical studies of the polymer stars were carried out using renormalization group [32–43] (see also Ref. [44] and references therein) and the field theoretical [45–47] approaches, extrapolation of exact enumerations [48–51], free energy minimization method [52–54], mean field [55–57] and scaling theories [58–66], as well as the density functional approach [67]. In general, the properties of polymers have been studied intensively in the past using computer simulations methods, such as molecular dynamics and Monte-Carlo methods [68–72]. These methods were also used to study the properties of the star polymers and a large number of corresponding studies have been published during the last decade (see Ref. [73] and references there in).

One of important properties of star polymers that affect their technological application is their shape. Conformational and shape properties of the star polymers, which include mean square radius of gyration and hydrodynamic radii, were studied experimentally [74–78]. The universal shape properties of the linear chain polymers in a form of a self-avoiding walk (SAW) were also studied recently via lattice modeling [22,79–86]. It was demonstrated that certain shape properties of polymer chains, similar to the scaling exponents, are universal and depend solely on dimensionality of the space d . This type of the approach appears to be very efficient and allows one to achieve very good configuration statistics by means of a relatively low computational cost. However, the lattice models are not able to easily account for the effects of chain stiffness, chain composition, the quality of a solvent, etc. On the other hand, atomistic first principal simulations [87], which can include all these features, require substantial amount of the computer time. Perhaps, the most adequate computer simulation method to be used, which is able to compromise between chemical versatility and computational efficiency, is the dissipative particle dynamics (DPD) method. Applications of this method to the case of star polymers are already present [88–94]. In particular, in the paper of Nardai and Zifferer [87], dilute solutions of linear star polymers have been studied using DPD simulations. On the other hand, in our previous paper [95] we applied the DPD method to investigate the shape characteristics of a linear polymer chain in a good solvent. We have shown that such shape properties of the chain as asphericity, prolateness and some other are universal. The paper may be regarded as an extension of our work [95] on shape properties of linear polymer chains aiming at systematic analysis of the combined impact of solvent quality and polymer topology of the polymer shape properties. The aim of this study is to apply the same analysis to the case of star polymers. The outline of the paper is as follows. Sec. 2 contains detailed description of the model star polymers and the properties of interest to be studied. Sec. 3 contains the results and their interest. Conclusions are given in Sec. 4.

2. The model, simulation approach and properties of interest

As already mentioned in Sec. 1, our study is based on the mesoscopic DPD simulation technique. In this approach, the monomers, as well as the solvent beads, represent respective groups of atoms. They are soft spheres of equal size, repulsive to each other. Therefore, the DPD technique enables one to consider both the effects of a star-like topology as well as solvent quality via explicit account of mesoscopic polymer-solvent and solvent-solvent interactions

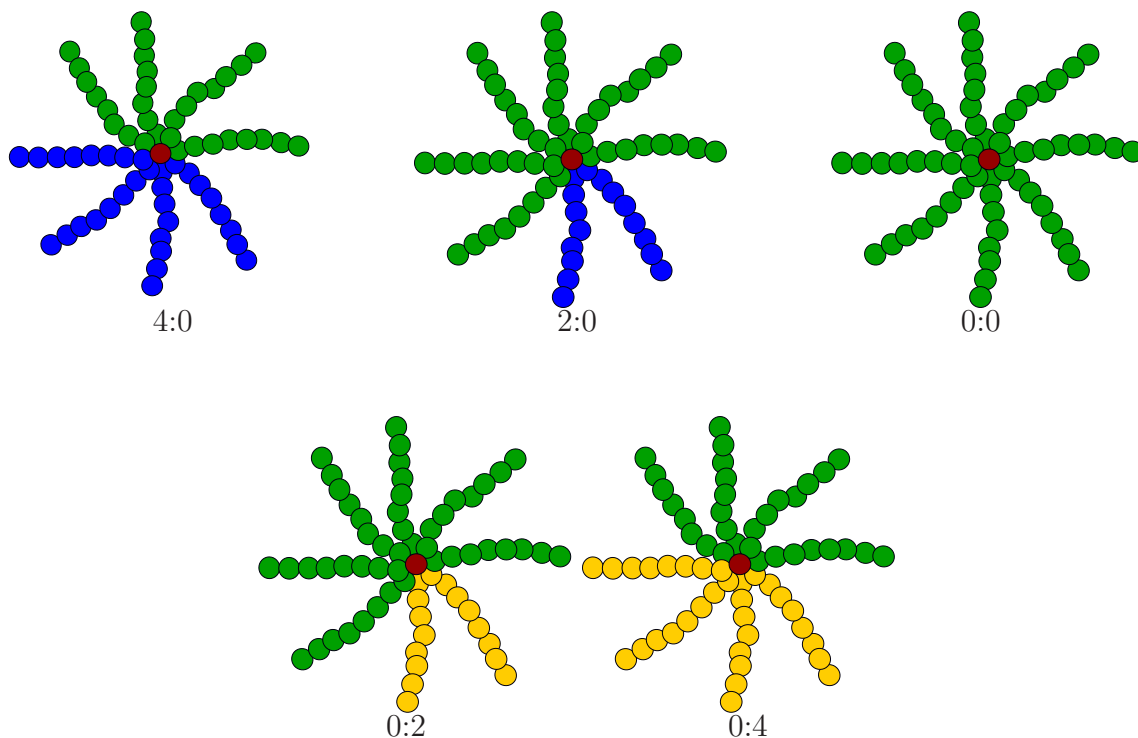


Figure 1. Sketches of polymer stars considered in this paper. Each star consists of $f_A + f_B + f_C = 8$ branches of equal length of $N_f = 8$ monomers attached to the central core (red sphere). f_A and f_B denotes the number of solvophilic and solvophobic branches, respectively, f_C stands for branches with variable solvophobicity. For the homogeneous star ($f_A = 0$, $f_B = 0$, further denoted as 0:0), all $f_C = 8$ branches have the same solvophobicity, that varies from the good solvent to bad solvent regime. For the heterogeneous stars (4:0, 2:0, 0:2, 0:4), the blue f_A branches do not change their solvophobicity remaining always solvophilic while the yellow f_B branches are always solvophobic, whereas solvophobicity of the green f_C branches varies.

We follow DPD method as formulated in Ref. [96]. The following reduced quantities are used: the length will be measured in units of the diameter of the soft bead, and the energy in units of $k_B T$. Here, k_B is the Boltzmann constant and T is the temperature. The monomers of each branch are connected via harmonic springs, which results in the force

$$\mathbf{F}_{ij}^B = -k\mathbf{x}_{ij}, \quad (1)$$

where $\mathbf{x}_{ij} = \mathbf{x}_i - \mathbf{x}_j$, \mathbf{x}_i and \mathbf{x}_j are the coordinates of i th and j th bead, respectively, and k is the spring constant. The total force acting on the i th bead from the j th one can be denoted as

$$\mathbf{F}_{ij} = \mathbf{F}_{ij}^C + \mathbf{F}_{ij}^D + \mathbf{F}_{ij}^R, \quad (2)$$

where \mathbf{F}_{ij}^C is the conservative force responsible for the repulsion between the beads, \mathbf{F}_{ij}^D is the dissipative force that defines the friction between them and the random force \mathbf{F}_{ij}^R works in pair with a dissipative force to thermostat the system. The expression for all these three contribution are given below [96]

$$\mathbf{F}_{ij}^C = \begin{cases} a(1 - x_{ij}) \frac{\mathbf{x}_{ij}}{x_{ij}}, & x_{ij} < 1, \\ 0, & x_{ij} \geq 1, \end{cases} \quad (3)$$

$$\mathbf{F}_{ij}^D = -\gamma w^D(x_{ij}) (\mathbf{x}_{ij} \cdot \mathbf{v}_{ij}) \frac{\mathbf{x}_{ij}}{x_{ij}^2}, \quad (4)$$

$$\mathbf{F}_{ij}^R = \sigma w^R(x_{ij}) \theta_{ij} \Delta t^{-1/2} \frac{\mathbf{x}_{ij}}{x_{ij}}, \quad (5)$$

where $x_{ij} = |\mathbf{x}_{ij}|$, $\mathbf{v}_{ij} = \mathbf{v}_i - \mathbf{v}_j$, \mathbf{v}_i is the velocity of the i th bead, a is the amplitude for the conservative repulsive force. The dissipative force has an amplitude γ and decays with distance according to the weight function $w^D(x_{ij})$. The amplitude for the random force is σ and the respective weight function is $w^R(x_{ij})$. θ_{ij} is the Gaussian random variable. As was shown by Español and Warren [97], to satisfy the detailed balance requirement, the amplitudes and weight functions for the dissipative and random forces should be interrelated: $\sigma^2 = 2\gamma$ and $w^D(x_{ij}) = [w^R(x_{ij})]^2$. Here we use quadratically decaying form for the weight functions:

$$w^D(x_{ij}) = [w^R(x_{ij})]^2 = \begin{cases} (1 - x_{ij})^2, & x_{ij} < 1, \\ 0, & x_{ij} \geq 1. \end{cases} \quad (6)$$

The reduced density of the system is defined as $\rho^* = (N + N_s)/V = 3$, where N_s is the number of solvent particles and V is system volume. The other parameters are chosen as follows: $\gamma = 6.75$, $\sigma = \sqrt{2\gamma} = 3.67$

Parameter a in the conservative force \mathbf{F}_{ij}^C defines maximum repulsion between two beads which occurs at their complete overlap, $x_{ij} = 0$. We consider three types of branches: solvophilic (beads of type A), solvophobic (beads of type B) and with variable solvophobicity (beads of type C). Their respective numbers are f_A , f_B and f_C . Each star type is denoted as $(f_A : f_B)$, and f_C is equal to $f_C = f - f_A - f_B$. The solvent beads are of type S . The values of the repulsion parameter a are chosen according to the bead types. Namely: $a_{AA} = a_{BB} = a_{CC} = a_{SS} = a_{AS} = 25$ and $a_{BS} = 40$. The value of a_{CS} is varied within the range from 25 (solvophilic branch) up to 40 (solvophobic branch). In what follows below, we have chosen to characterize shape of star polymers in terms of their radius of gyration and asphericity. The latter can be obtained from the eigenvalues of the gyration tensor \mathbf{Q} defined as [20, 21]:

$$Q_{\alpha\beta} = \frac{1}{N} \sum_{n=1}^N (x_n^\alpha - X^\alpha)(x_n^\beta - X^\beta) \quad \alpha, \beta = 1, 2, 3, \quad (7)$$

where N is the number of monomers of a star polymer, x_n^α stands for the set of the Cartesian coordinates of n th monomer: $\mathbf{x}_n = (x_n^1, x_n^2, x_n^3)$, and $X^\alpha = \frac{1}{N} \sum_{n=1}^N x_n^\alpha$ are the coordinates of the center of mass for the star polymer. Its eigenvectors define the axes of a local frame of a star polymer and the mass distribution of the latter along each axis is given by the respective eigenvalues λ_i , $i = 1, 2, 3$. The trace of \mathbf{Q} is an invariant with respect to rotations and is equal to an instantaneous squared gyration radius of the star polymer

$$R_g^2 = \text{Tr } \mathbf{Q} = \sum_{i=1}^3 \lambda_i = 3\bar{\lambda} \quad (8)$$

Here, the arithmetic mean of three eigenvalues, $\bar{\lambda}$, is introduced to simplify the forthcoming expressions. The asphericity A [22, 79, 81, 86] for the three-dimensional case is defined as

$$A = \frac{1}{6} \frac{\sum_{i=1}^3 (\lambda_i - \bar{\lambda})^2}{\bar{\lambda}^2}. \quad (9)$$

By definition, an inequality holds: $0 \leq A \leq 1$ [86]. The asphericity equals zero for an ideally spherical shape, when all eigenvalues are equal: $\lambda_i = \bar{\lambda}$. On the other extreme, an asphericity of a rod, when all eigenvalues but one vanish, $A = 1$. In the course of simulations, the instantaneous value A is then averaged over time trajectory of simulations, this averaged value is denoted as $\langle A \rangle$.

3. Results

As already discussed in Sec. 2, we consider four types of heterogeneous stars and a homogeneous star copolymer, see Fig. 1. The linear size of a cubic simulation box is chosen to be at least four gyration radius of a single branch in a coiled conformation. For each heterogeneous star we perform $2 \cdot 10^6$ DPD steps, whereas for a homogeneous star the simulation length is $6 \cdot 10^6$ DPD steps, for each considered value of a_{CS} . The time step is $\Delta t^* = 0.04$. To estimate statistical errors of particular characteristic x , the simulation time trajectory is divided into four equal intervals. In each i th interval we calculate its partial simple average value $\langle x \rangle^{[i]}$ and the histogram for its distribution $P^{[i]}(x)$.

First we analyse the value of the gyration radius R_g for a star polymer depending on the solvent quality. The latter was tuned by the choice of a_{CS} , from the good solvent case ($a_{CS} = 25$) to the bad one ($a_{CS} = 40$), see Fig. 2. Let us consider the change undergone by R_g for the case of the homogeneous star (0:0), when a_{CS} increases from 25 to 40. This change drives the conformation of all the branches from a coiled state to the collapsed one. As a consequence, the R_g decreases smoothly from 5.8 down to 2. For the heterogeneous stars with fixed solvophilic branches (4 : 0 and 2 : 0), the R_g value at $a_{CS} = 25$ is, obviously, the same as the one for the homogeneous star. But at $a_{CS} = 40$ the gyration radius for both (4 : 0) and (2 : 0) stars have higher magnitude due to the fact that f_A branches are still in a coiled state, whereas the other f_C branches are

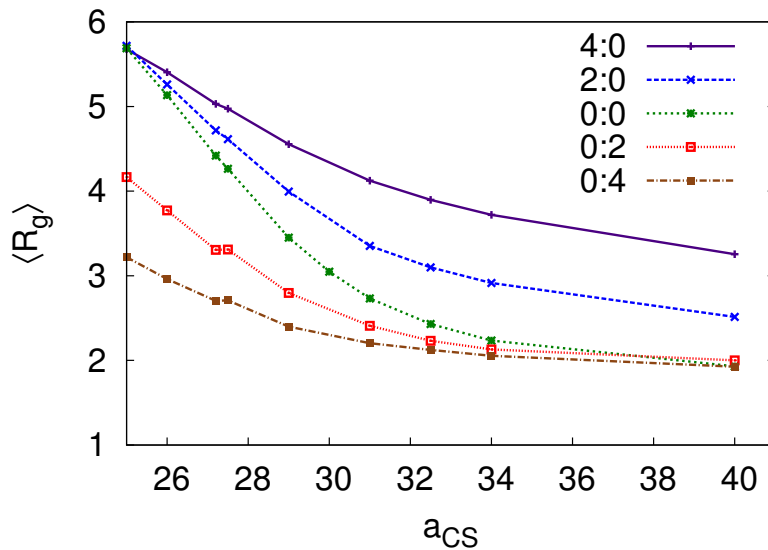


Figure 2. Mean gyration radius $\langle R_g \rangle$ of the $(f_A : f_B)$ polymer star as a function of a_{CS} . Here f_A is a number of solvophilic branches and f_B is a number of solvophobic branches. The rest $f_C = f - f_A - f_B$ branches have variable solvophilicity. The a_{CS} parameter discriminates between good ($a_{CS} = 25$) and bad ($a_{CS} = 40$) solvent quality for the f_C branches. Green line corresponds to a homogeneous star when $f_C = f$, marked as $(0 : 0)$. Here the gyration radius is expressed in the units σ which is the diameter of one monomer.

in a collapsed state. On contrary, heterogeneous stars with fixed solvophobic branches $(0 : 2)$ and $(0 : 4)$ have the same value of R_g at $a_{CS} = 40$ as the homogeneous star and a lower value at $a_{CS} = 25$. This is, obviously, due to the fact that at $a_{CS} = 25$ only f_C branches are in a coil state, whereas the other f_B branches are always in a collapsed state.

In the DPD method all the beads are soft and can overlap, unlike for the hard spheres model. To quantify this effect, we analysed the packing fraction ϕ of beads depending on the solvent quality, see Fig. 3. It is given by

$$\phi = \frac{N_b \frac{4}{3} \pi r^3}{V_{glob}} \quad (10)$$

where N_b is the number of beads in a star polymer, r is the radius of a single bead and V_{glob} is the volume occupied by star polymer. This volume can be expressed *via* the expression $V_{glob} = \frac{4}{3} \pi R^3$, where R is the radius of an equivalent sphere with the same volume as that of a star polymer. We estimate R from its relation to the gyration radius R_g . As the first approximation, one can take the relation $R = \sqrt{\frac{5}{3}} R_g$ which holds for a solid spheres. We also display in Fig. 3 the packing fractions that relate to two limiting cases. These are marked as (a): the case when all the branches are in a fully stretched conformation and (b), when the star polymer comprises a compact object of tightly packed hard spheres. In the good solvent regime at $a_{CS} = 25$, the packing fraction is $\phi \approx 0.28$ which is close to the case (a). At $a_{CS} = 30$, the packing fraction crosses the

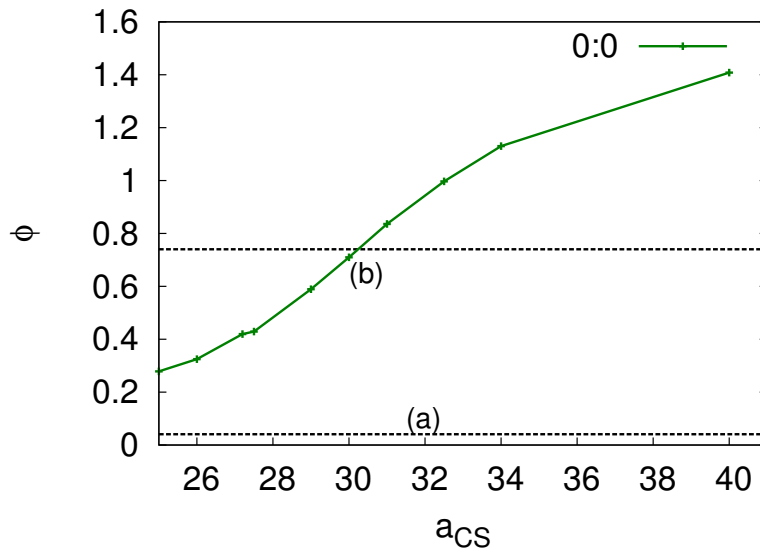


Figure 3. Solid line: packing fraction ϕ of the homogeneous star (0 : 0) at various a_{CS} , the solvophobicity of its beads. Dashed lines: packing fractions of the case when all branches are fully stretched (a) and when they are tightly packed (b)

line (b). With an increase of a_{CS} the packing fraction increases, and in the bad solvent regime at $a_{CS} = 40$, ϕ is equal to 1.4. It is indicating severe beads overlap, and, hence highly compressed state of the star polymer.

Let us switch our attention to the asphericity of the stars. The histograms $P^{[i]}(A)$ for the distribution of asphericity in each $[i]$ th interval A are presented in Fig. 4 for the case of homogeneous star at $a_{CS} = 27.5$. This value was estimated earlier in Ref. [87] as the one providing approximately the θ -conditions for similar model of a star polymer. We observe that the data points obtained for each $P^{[i]}(A)$ follow the same curve. The shape of this curve, similarly to the case of linear polymer chain [95], can be approximated well by the Lhuillier-type distribution:

$$P_L(A) = B \exp \left[- \left(\frac{A'}{A} \right)^{\epsilon_1} - \left(\frac{A}{A'} \right)^{\epsilon_2} \right], \quad A_{max} = A' \left(\frac{\epsilon_1}{\epsilon_2} \right)^{\frac{1}{\epsilon_1 + \epsilon_2}}. \quad (11)$$

Here A_{max} is the position of the maximum for the $P_L(A)$ and B, A', ϵ_1 and ϵ_2 are fitting parameters. We perform the separate fit for each $P^{[i]}(A)$ to the form Eq. (11) resulting in a set of parameters $B^{[i]}, A'^{[i]}, \epsilon_1^{[i]}, \epsilon_2^{[i]}$ and $A_{max}^{[i]}$. The sets provide both the respective averages for each of these parameters, as well as their standard deviations evaluated within the set. The same procedure is used for all values of $a_{CS} = 25 - 40$. The results for the simple average of the asphericity $\langle A \rangle$, and the average position of the maximum A_{max} , alongside with their respective errors are shown in Fig. 5. Similarly to the data shown in Fig. 4, the magnitude of $\langle A \rangle$ is higher than that for A_{max} . However, the changes undergone by both characteristics with the variation of a_{CS} are very similar. Namely, both increase within the interval $25 < a_{CS} < 29$, peak at approximately $a_{CS} = 29$ and then both decay. For both characteristics we observe a maximum at the interval

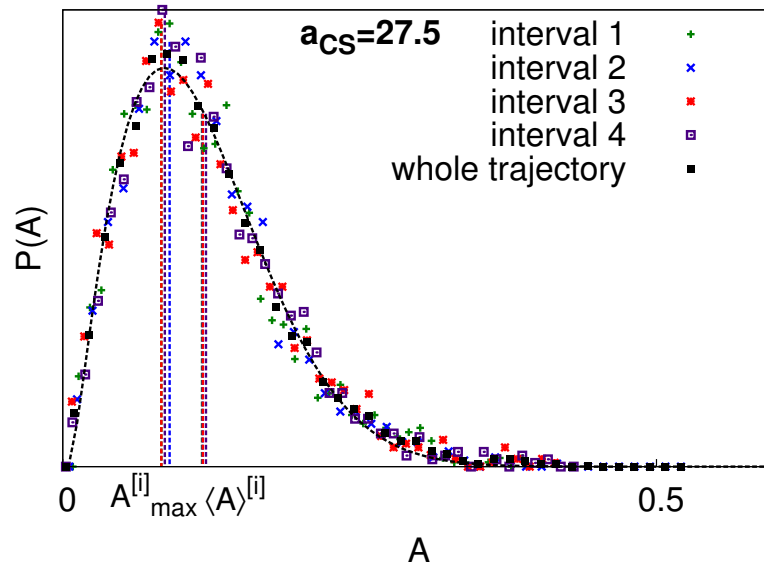


Figure 4. Distribution of the asphericity A of a homogeneous star at solvent quality $a_{CS} = 27.5$ for the intervals 1: $0 < N_{stp} < 15 \cdot 10^5$, 2: $15 \cdot 10^5 < N_{stp} < 3 \cdot 10^6$, 3: $3 \cdot 10^6 < N_{stp} < 45 \cdot 10^5$, 4: $45 \cdot 10^5 < N_{stp} < 6 \cdot 10^6$, as well as for the whole simulation $0 < N_{stp} < 6 \cdot 10^6$. Black curve is fitting according to Eq. 11

$27 < a_{CS} < 29$. This interval contains the value $a_{CS} = 27.5$ estimated as a θ -point by Nardai and Zifferer [87], for the same simulations model. Below we attempt to clarify the reason for this maxima.

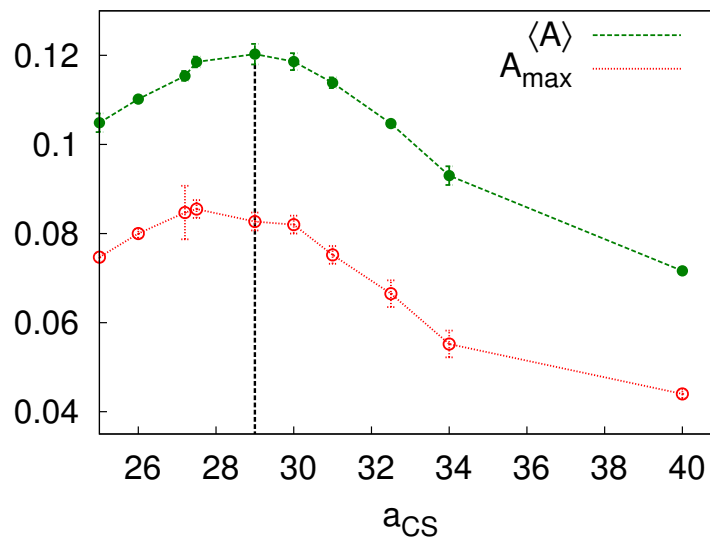


Figure 5. Plot of the asphericity of a homogeneous star as a function of the solvophobicity of its beads a_{CS} . Here $\langle A \rangle$ and A_{max} are the mean and maximal values of A is found from the distribution (11).

To clarify this peculiarity of the asphericity at the θ -condition, we will consider the

asphericity of the heterogeneous stars, depicted in Fig. 6. The cases (2 : 0) and (4 : 0) at $a_{CS} = 25$ are characterized by all the branches being in a coiled state, similarly to the case (0 : 0) at the same a_{CS} . Hence, the same value of $\langle A \rangle = 0.105$ is observed in all cases mentioned above. With the a_{CS} value approaching 40, the (0 : 2) and (0 : 4) stars at $a_{CS} = 40$ have all their branches collapsed. Again, this mimics the case of (0 : 0) star at $a_{CS} = 40$. Therefore, not surprisingly, the $\langle A \rangle$ values for those stars are close to the respective value of 0.075 for the homogeneous star (cf. Figs. 5 and 6). However, cases (0 : 2) and (0 : 4) at $a_{CS} = 25$ both have a higher asphericity value of $\langle A \rangle = 0.12$, the same as for the case (2 : 0) and (4 : 0) at $a_{CS} = 40$. This higher value of $\langle A \rangle$ is observed due to the fact that in all these cases some branches are in a coiled state and the other branches are collapsed. It is instructive to note that the same value $\langle A \rangle = 0.12$ is also observed for the homogeneous star (0 : 0) in the interval $27 < a_{CS} < 29$. This leads us to the idea that the maxima of $\langle A \rangle$ for the (0 : 0) star, observed in this interval might be related to the coexistence of both coiled and collapsed configurations of the branches, in a θ -solvent regime.

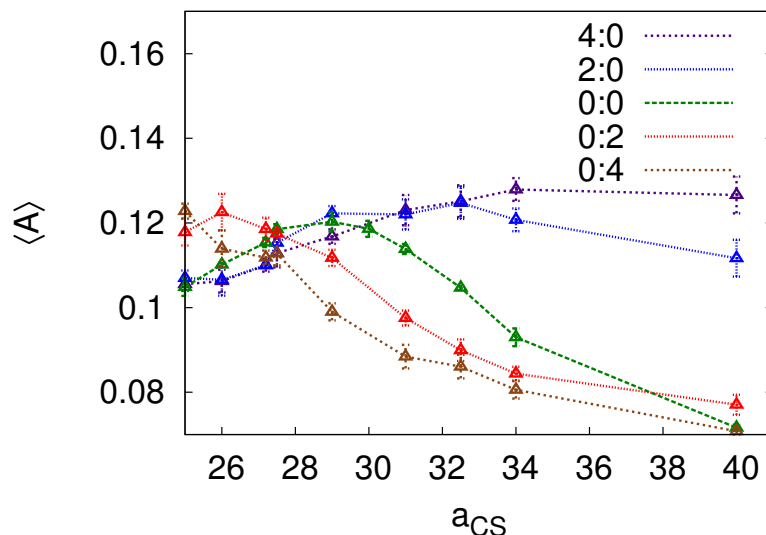


Figure 6. Asphericity A of the $(f_A : f_B)$ polymer star as a function of a_{CS} , the solvophobicity of the C beads. Here f_A is a number of solvophilic branches and f_B is a number of solvophobic branches. Factor a_{CS} discriminates between good ($a_{CS} = 25$) and bad ($a_{CS} = 40$) solvent quality. Green line corresponds to a homogeneous star with all branches of changing solubility (0 : 0).

There different conditions for the individual branches of homogeneous star polymer, namely the cases of good, bad and the θ -solvent, are illustrated in Fig. 7. These cases are considered in terms of the interplay between the enthalpic, U , and the entropic S , contributions to the free energy $F = U - TS$, with T being the temperature. The case of a good solvent ($a_{CS} = 25$) is displayed in Fig. 7(a). Here all the branches are in a coiled state and are surrounded by a solvation shell. In this case, there is an effective repulsion

between branches, leading to the non-zero enthalpy contribution U . For the case of a bad solvent, Fig. 7(c), the branches strongly repel each other strongly by a solvent, leading to their collapse, this is interpreted as the effective solvent-mediated attraction between branches. In this case, the contribution of U to the free energy is also non-zero. The intermediate case, where polymer is in the θ -solvent condition, is characterized by vanishing of the enthalpy contribution U and the free energy is driven now only by the entropy. As a consequence, all branches turn into the ideal chains, their conformations are uncorrelated and each one can be interpreted as a random walk. This may lead to the coexistence of both coiled and collapsed configurations of individual chains, as illustrated schematically in Fig. 7(b).

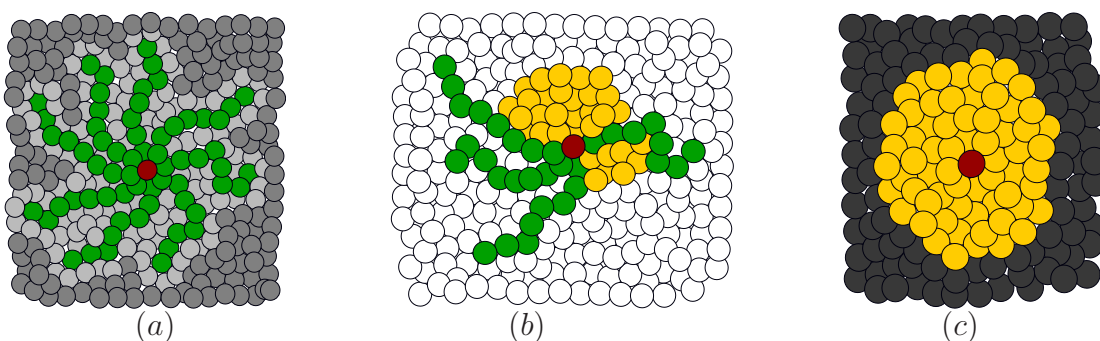


Figure 7. Schematic illustration for the coformation of individual branches of homogeneous star polymer (0 : 0) in various regimes. (a) good solvent, (b) θ -condition and (c) bad solvent.

To confirm this interpretation of the behavior of the star polymer in the θ -solvent we conducted the analyses of the configurations of individual branches. The histogram for the distribution $p(\alpha)$ for the asphericity α of individual branches is illustrated in Fig. 8 for the homogeneous star at $a_{CS} = 25, 27.5, 30$ and 40 . The general shape of this distribution changes essentially when a_{AC} varies from 25 to 40. In general, it shows the presence of two maxima. Therefore, we fitted the data by a double Gaussian distribution:

$$p(a) = A' \exp \left[-\left(\frac{x - \alpha'}{\sigma'} \right)^2 \right] + A'' \exp \left[-\left(\frac{x - \alpha''}{\sigma''} \right)^2 \right], \quad (12)$$

where A' and A'' are respective weights, α' and α'' - respective position of two maxima, σ_1 and σ_2 are the respective dispersions. The results of the fits for A' , A'' , α' and α'' are collected in Tab. 1. Based on these results and the shape of the $p(a)$ distribution, we can deduct the following conclusion. In all cases $a_{CS} = 25 - 40$ we see the coexistence of typical conformations, one with lower asphericity, $\alpha' \approx 0.2 - 0.26$, and another one with a higher asphericity, $\alpha'' \approx 0.4 - 0.56$. For the case of $a_{CS} = 40$ low asphericity conformations prevail, as far as $A' > A''$. Here all branches are in the collapsed state and the distribution has one maximum near $\alpha' = 0.25$. On the contrary, at $a_{CS} = 25$ we have $A' < A''$, hence the conformations with higher asphericity prevail. This is due to the branches being predominately found in a coiled state. At $a_{CS} = 27.5 - 30$

a_{CS}	25	27.5	30	40
α'	0.257	0.225	0.212	0.205
A'	1.056	1.266	1.289	1.811
α''	0.555	0.512	0.435	0.402
A''	1.683	1.617	1.587	1.514

Table 1. α' and α'' are the positions of the maxima, A' and A'' are the respective weights of the Gaussian distributions and σ' and σ'' are the respective dispersion.

the distribution clearly has two maxima. This evidences the coexistence of rather collapsed conformations with those that are more close to a coiled state. Hence, at the θ condition of a star polymer, there is much higher degree of the solvent regime for conformational freedom of its branches, and as a consequence, by a coexistence of more coiled conformation with the ones closer to a collapsed state. This explains the maximum for the average asphericity $\langle A \rangle$ as observed in Fig. 5.

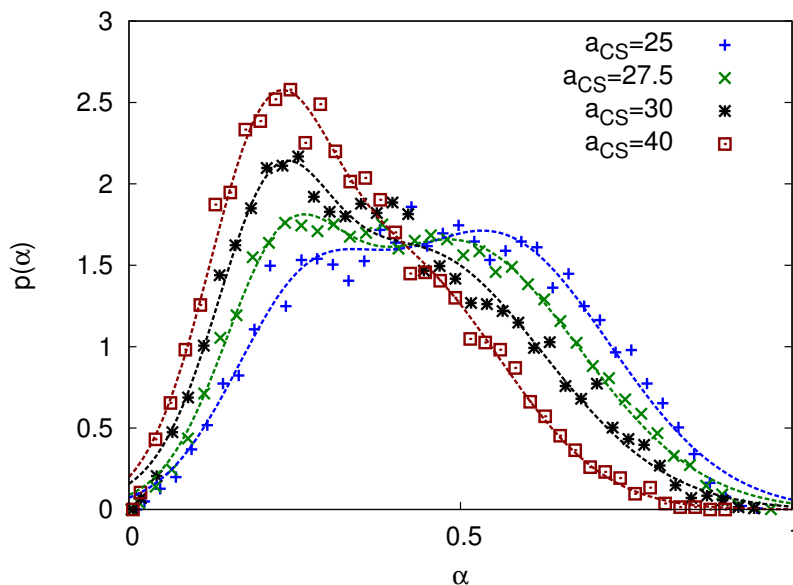


Figure 8. Distribution of asphericity $p(\alpha)$ of individual branches of a homogeneous star at various solvophobicity of its branches a_{CS} .

4. Conclusions

We have analysed the shape characteristics of the coarse-grained heterogeneous and homogeneous star-like polymers at various solvent quality using the DPD simulations. The heterogeneous star is characterized by different solvophobicity of its individual branches. The solvent quality was tuned by varying the parameter a_{CS} for the repulsive conservative force of the branches with variable solvophobicity. For homogeneous and four types of heterogeneous star polymers, the gyration radius decreases with the

increase of the repulsion parameter a_{CS} indicating a collapsed state for the part or all their branches. The packing fraction ϕ at $a_{CS} = 30$ is close to the packing fraction of the hexagonally packed hard spheres. We found an interesting effect that, upon the change of solvent properties, the asphericity of a homogeneous star reaches its maximum value when the solvent is near θ -point. The effect is explained by the interplay between the enthalpic and entropic contributions to the free energy. In particular, at the θ -point condition, the enthalpic contribution vanishes and the branch conformation are driven exclusively by the entropy. This provides means for the wider spectra of possible conformations from collapsed to the coiled ones. We check this explanation by the analyses of the asphericity of the individual branches. Their distribution near θ -condition has two maxima, which is well fitted by double Gaussian distribution. This confirms the coexistence of two types of conformation, namely, more coiled and more collapsed ones. An extension of this analyses to the case of aggregation of star-like polymers into micelles which has applications for the drug delivery systems will be the subject of the forthcoming paper.

5. Acknowledgements

This work was supported in part by FP7 EU IRSES project No. 612707 "Dynamics of and in Complex Systems" and No. 612669 "Structure and Evolution of Complex Systems with Applications in Physics and Life Science". J.I. acknowledges Alexander Blumen for stimulating discussions towards the interpretation of the result.

- [1] Schaeffgen J R and Flory P J 1948 *Journal of the American Chemical Society* **70** 2709–2718.
- [2] Morton M, Helminiak T E, Gaskary S D and Bueche F 1962 *Journal of Polymer Science* **57** 471–482.
- [3] Mishra M and Kobayashi S 1999 *Star and hyperbranched polymers* vol 53 (CRC Press).
- [4] Hadjichristidis N, Pitsikalis M, Pispas S and Iatrou H 2001 *Chemical Reviews* **101** 3747–3792.
- [5] Hadjichristidis N, Pitsikalis M, Iatrou H, Driva P, Sakellariou G and Chatzichristidi M 2012 29–111.
- [6] Khanna K, Varshney S and Kakkar A 2010 *Polymer Chemistry* **1** 1171.
- [7] Gast A P 1996 *Langmuir* **12** 4060–4067
- [8] Grest G, Fetters L, Huang J and Richter D 1996 *Polymeric Systems; Prigogine, I.; Rice, SA, Eds.; Wiley: New York* **94** 67–163
- [9] Likos C N, Löwen H, Watzlawek M, Abbas B, Jucknischke O, Allgaier J and Richter D 1998 *Physical Review Letters* **80** 4450–4453
- [10] Witten T A and Pincus P A 1986 *Macromolecules* **19** 2509–2513
- [11] Sikorski A 1993 *Polymer* **34** 1271–1281
- [12] Factor B J, Russell T P, Smith B A, Fetters L J, Bauer B J and Han C C 1990 *Macromolecules* **23** 4452–4455
- [13] Vlassopoulos D, Pakula T, Fytas G, Pitsikalis M and Hadjichristidis N 1999 *The Journal of Chemical Physics* **111** 1760–1764
- [14] Grest G S, Kremer K, Milner S T and Witten T A 1989 *Macromolecules* **22** 1904–1910
- [15] Su S J, Denny M S and Kovac J 1991 *Macromolecules* **24** 917–923
- [16] Su S J and Kovac J 1992 *The Journal of Physical Chemistry* **96**
- [17] Stratinf P and Wiegell F 1994 *International Journal of Modern Physics B*
- [18] Sikorski A and Romiszowski P 1999 *Macromolecular theory and simulations* **8** 103–109
- [19] Ganazzoli F, Allegra G, Colombo E and Vitis M D 1995 *Macromolecules*
- [20] Šolc K 1971 *The Journal of Chemical Physics* **54** 2756
- [21] Šolc K and Stockmayer W H 1971 *The Journal of Chemical Physics* **55** 335
- [22] Zifferer G 1999 *The Journal of Chemical Physics* **110** 4668–4677
- [23] Xue L, Agarwal U S and Lemstra P J 2005 *Macromolecules* **38**
- [24] Lohse D J, Milner S T, Fetters L J, Xenidou M, Hadjichristidis N, Mendelson R A, García-Franco C A and Lyon M K 2002 *Macromolecules* **35** 3066–3075
- [25] Schober B J, Vickerman R J, Leeb O D, Dimitrakisa W J and Gajanayakec A 2008 Controlled architecture viscosity modifiers for driveline fluids: Enhanced fuel efficiency and wear protection *Proceedings of the 14th Annual Fuels Lubes Asia Conference*
- [26] Knoll K and Nießner N 1998 *Macromolecular Symposia* **132**
- [27] Maness K M, Masui H, Wightman R M and Murray R W 1997 *Journal of the American Chemical Society* **119** 3987–3993
- [28] Likos and Harreis 2002 *Condensed Matter Physics* **5** 173
- [29] Hecht S, Ihre H and Fréchet J M J 1999 *Journal of the American Chemical Society* **121** 9239–9240
- [30] Heyes C D, Groll J, Möller M and Nienhaus G U 2007 *Mol. BioSyst* **3** 419–430
- [31] James H P, John R, Alex A and Anoop K 2014 *Acta Pharmaceutica Sinica B* **4** 120–127
- [32] Douglas J F, Roovers J and Freed K F 1990 *Macromolecules* **23** 4168–4180
- [33] Shiwa Y, Oono Y and Baldwin P R 1990 *Modern Physics Letters B* **04** 1421–1428
- [34] Merkle G, Burchard W, Lutz P, Freed K F and Gao J 1993 *Macromolecules* **26** 2736–2742
- [35] Zhu S 1998 *Macromolecules* **31** 7519–7527
- [36] Vlahos C H, Horta A and Freire J J 1992 *Macromolecules* **25**
- [37] Duplantier B 1986 *Physical Review Letters* **57** 941–944
- [38] Ohno K and Binder K 1991 *The Journal of Chemical Physics* **95**
- [39] Ohno K and Binder K 1988 *Journal de Physique* **49** 1329–1351
- [40] Miyake A and Freed K F 1983 *Macromolecules* **16** 1228–1241
- [41] Miyake A and Freed K F 1984 *Macromolecules* **17** 678–683
- [42] Vlahos C H and Kosmas M K 1987 *Journal of Physics A: Mathematical and General* **20** 1471–1483

- [43] von Ferber C and Holovatch Y 1997 *Physical Review E* **56** 6370–6386
- [44] von Ferber C and Holovatch Y 1999 *Physical Review E* **59** 6914–6923
- [45] Chujo Y, Naka A, Krämer M, Sada K and Saegusa T 1995 *Journal of Macromolecular Science, Part A* **32** 1213–1223
- [46] Okamoto S, Hasegawa H, Hashimoto T, Fujimoto T, Zhang H, Kazama T, Takano A and Isono Y 1997 *Polymer* **38** 5275–5281
- [47] Knoll K and Nießner N 1998 Styrolux and styroflex from transparent high impact polystyrene to new thermoplastic elastomers: Syntheses, applications and blends with other styrene based polymers *Macromolecular Symposia* vol 132 (Wiley Online Library) pp 231–243
- [48] Lipson J E G, Whittington S G, Wilkinson M K, Martin J L and Gaunt D S 1985 *Journal of Physics A: Mathematical and General* **18** L469–L473
- [49] Wilkinson M K, Gaunt D S, Lipson J E G and Whittington S G 1986 *Journal of Physics A: Mathematical and General* **19** 789–796
- [50] Barrett A J and Tremain D L 1987 *Macromolecules* **20** 1687–1692
- [51] Colby S A, Gaunt D S, Torrie G M and Whittington S G 1987 *Journal of Physics A: Mathematical and General* **20** L515–L520
- [52] Ganazzoli F and Allegra G 1990 *Macromolecules* **23** 262–267
- [53] Ganazzoli F, Fontelos M A and Allegra G 1991 *Polymer* **32** 170–180
- [54] Ganazzoli F 1992 *Macromolecules* **25** 7357–7364
- [55] Boothroyd A T and Ball R C 1990 *Macromolecules* **23** 1729–1734
- [56] Boothroyd A T and Fetters L J 1991 *Macromolecules* **24** 5215–5217
- [57] Irvine D J, Mayes A M and Griffith-Cima L 1996 *Macromolecules* **29**
- [58] Ohno K and Binder K 1991 *The Journal of Chemical Physics* **95**
- [59] Ohno K and Binder K 1991 *The Journal of Chemical Physics* **95**
- [60] Halperin A and Joanny J F 1991 *Journal de Physique II* **1** 623–636
- [61] Raphael E, Pincus P and Fredrickson G H 1993 *Macromolecules* **26** 1996–2006
- [62] Daoud M and Cotton J 1982 *Journal de Physique* **43** 531–538
- [63] Birshtein T and Zhulina E 1984 *Polymer* **25** 1453–1461
- [64] Duplantier B 1986 *Physical Review Letters* **57** 941–944
- [65] Duplantier B and Saleur H 1986 *Physical Review Letters* **57** 3179–3182
- [66] Duplantier B and Saleur H 1987 *Physical Review Letters* **59** 539–542
- [67] Groh B and Schmidt M 2001 *The Journal of Chemical Physics* **114** 5450–5456
- [68] Rey A, Freire J J, Bishop M and Clarke J H R 1992 *Macromolecules* **25** 1311–1315
- [69] Binder K 1995 *Monte Carlo and molecular dynamics simulations in polymer science* (Oxford University Press)
- [70] 2002 Preface to the second edition *Understanding Molecular Simulation* (Elsevier) pp xiii–xiv
- [71] Kotelyanskii M and Theodorou D N 2004 *Simulation methods for polymers* (CRC Press)
- [72] Galiatsatos V 2005 *Molecular simulation methods for predicting polymer properties* (Wiley-Interscience)
- [73] von Ferber and YuHolovatch 2002 *Condensed Matter Physics* **5** 3
- [74] Allgaier J, Martin K, Räder H J and Müllen K 1999 *Macromolecules* **32** 3190–3194
- [75] Feng X S and Pan C Y 2002 *Macromolecules* **35** 2084–2089
- [76] Roovers J E L and Bywater S 1972 *Macromolecules* **5** 384–388
- [77] Roovers J E L and Bywater S 1974 *Macromolecules* **7** 443–449
- [78] Zhou L L, Hadjichristidis N, Toporowski P M and Roovers J 1992 *Rubber Chemistry and Technology* **65** 303–314
- [79] Aronovitz J and Nelson D 1986 *J. Phys. France* **47** 1445–1456
- [80] Cannon J W, Aronovitz J A and Goldbart P 1991 *J. Phys. I France* **1**
- [81] Zifferer G 1999 *Macromolecular Theory and Simulations* **8** 433–462
- [82] Jagodzinski O, Eisenriegler E and Kremer K 1992 *J. Phys. I France* **2** 2243–2279
- [83] Bishop M and Saltiel C J 1988 *The Journal of Chemical Physics* **88** 6594

- [84] Benhamou M and Mahoux G 1985 *Journal de Physique Lettres* **46** 689–693
- [85] Diehl H W and Eisenriegler E 1989 *J. Phys. A: Math. Gen.* **22** L87–L91
- [86] Blavatska V, von Ferber C and Holovatch Y 2011 *Condensed Matter Physics* **14** 33701
- [87] Nardai M M and Zifferer G 2009 *The Journal of Chemical Physics* **131** 124903
- [88] Qian H J, Chen L J, Lu Z Y, Li Z S and Sun C C 2006 *The Journal of Chemical Physics* **124** 014903
- [89] van Vliet R E, Hoefsloot H C and Iedema P D 2003 *Polymer* **44** 1757–1763
- [90] Ilnytskyi J M and Holovatch Y 2007 *Condensed Matter Physics* **10** 539
- [91] Xia J and Zhong C 2006 *Macromolecular Rapid Communications* **27** 1110–1114
- [92] Chou S H, Tsao H K and Sheng Y J 2006 *The Journal of Chemical Physics* **125** 194903
- [93] Sheng Y J, Nung C H and Tsao H K 2006 *The Journal of Physical Chemistry B* **110** 21643–21650
- [94] Español P and Warren P B 2017 *The Journal of Chemical Physics* **146** 150901
- [95] Kalyuzhnyi O, Ilnytskyi J M, Holovatch Y and von Ferber C 2016 *Journal of Physics: Condensed Matter* **28** 505101
- [96] Groot R D and Warren P B 1997 *The Journal of Chemical Physics* **107** 4423
- [97] Español P and Warren P 1995 *Europhysics Letters (EPL)* **30** 191–196